

# Synthesis of self-healing Smart Epoxy and Polyurethane Coating by Encapsulation of Olive Leaf Extract as Corrosion Inhibitor

Zahra Jamshidnejad\*, Abdollah Afshar, Mohammad Amin RazmjooKhallari

Department of Materials Science and Engineering, Sharif University of Technology Address: Azadi Avenue, 14588 Tehran, Iran

\*E-mail: [Zahrajamshidnejad@yahoo.com](mailto:Zahrajamshidnejad@yahoo.com)

*Received:* 28 August 2018 / *Accepted:* 8 October 2018 / *Published:* 5 November 2018

---

Self-healing coatings with the ability of recovering damaged areas, have a high potential application in corrosion prevention, because of high reliability and cost reductions. In this research, fabrication and characterization of epoxy and urethane based self-healing coatings by encapsulation of olive leaf extract as corrosion inhibitor are investigated. HOPDMS and PDES were used as healing agents in urethane shelled capsules. Moreover, olive leaf extract was added to the healing capsules to further increase the corrosion protection of the coating. By means of polarization and electrochemical impedance spectroscopy tests, it was proved that the olive leaf extract is an effective corrosion inhibitor for steel in chloride solutions, with an inhibition efficiency of about 80% for ethanol extracted inhibitor at 300 ppm. Submicron capsules containing inhibitor and healing agents were fabricated by simultaneous agitation and sonication, and were characterized by SEM, EDS and FTIR analyzes. Finally, the self-healing ability of the coatings containing 3,4, and 5 percent of capsules were studied, and it was found out that with increasing of capsules content of the coating, the corrosion protection improves, so that in a coating with 5 wt% of capsules, no evidence of corrosion was observed in the adjacent area of a damage.

---

**Keywords:** corrosion; self-healing coating; olive leaf extract; green inhibitor;

## 1. INTRODUCTION

Carbon steel is one of the most important engineering materials in industrial applications. However, its low corrosion resistance limits the service lifetime of steel parts and increases the maintenance costs. Application of organic coatings is one of the main means of steel protection from corrosive environments. An adhesive organic coating can protect the substrate metal by acting as a barrier layer on the top surface. However, if the coating is damaged, the substrate will be in contact

with the corrosive agents and local corrosion of the metal will happen. Moreover, formation of micro cracks in the coating can lead to disbonding of the coating from metal surface which further increases the corrosion rate of the metal [1-3]. Therefore, the risk of coating damage and its consequences, should be taken into account when choosing an organic coating for corrosion protection.

Self-healing organic coatings are specially developed to overcome the problems associated with coating damage. These coatings decrease the risk of substrate corrosion by recovering itself when damaged [4]. This feature is especially important when the coated surface is hard to inspect and repair, and it can greatly reduce the maintenance costs [2,5]. The self-healing feature can be achieved by various mechanisms. One of the most common method is embedding healing materials inside the coating in form of capsules. These capsules consist of a solid shell, and a core that contain healing material. When the solid shell tears due to mechanical damage to the coating, the healing material inside the shell is released which then polymerizes and heals the damaged area [3,6]. A wide range of healing agents including Tung oil [2], organic silane [7], linseed oil [8,9], and rapeseed oil [10] have been investigated.

The quality of the coating can be characterized by optical and scanning electron microscopy. Moreover, the self-healing feature can be investigated by scanning electrochemical microscopy (SECM) and electrochemical impedance spectroscopy [1,9,11].

Further protection improvement in self-healing coatings can be achieved by embedding inhibitors into the coating to protect the substrate metal against local corrosion damages [12]. Yakubi[13] injected sodium benzoate into nano-pores of a polymeric coating in order to enhance its corrosion protection. Furthermore, addition of benzotriazole to nanoporous Titania was also studied by Lamaka[14]. Nevertheless, there is no evidence of the effectiveness of inhibitors embedded in self-healing polymeric coatings. Potential environmental damages associated with corrosion inhibitor released from the coatings, is another issue that must be taken into consideration.

While industrial corrosion inhibitors such as chromates can have harmful effects on environment, green inhibitors can be a harmless alternative [15,16]. Extracts of some plant leaves, roots and seeds are proven to have strong corrosion inhibition effects while being environment friendly. Various types of plant sources have been investigated for this purpose including Opuntia extract [15], Phyllanthusamarus[17], fenugreek leaves [18], olive leaves [16,19], Thym leaves extract [12], ginko leaves [20], Pennyroyal oil [21] and papaya seeds [22], with olive leaf extract are one of the best options due to its low cost, availability and high corrosion inhibition efficiency in various environments [16,19]. Therefore, the olive leaves extract can be a reasonable choice for embedding into the self-healing polymeric base coating. To the best of our knowledge there are no reports on embedding olive leaves extract as inhibitor into self-healing coatings.

In this study, the inhibition effect of olive leaf extracts for protection of carbon steel in 0.6 M NaCl is investigated. The preparation and characterization of submicron-capsules containing both the olive leaf extract and healing agent is discussed, and corrosion protection and self-healing properties of epoxy and polyurethane coatings containing submicron capsules is studied.

## 2. MATERIALS AND PROCEDURE

### 2.1 Substrate

Test specimens cut with dimensions of 10 mm × 10 mm × 3 mm from A307 steel pipe with chemical composition according to Table 1, were prepared. The specimens were mechanically polished up to 800 grit, then rinsed with distilled water and acetone and then air dried.

**Table 1.** Chemical composition of A37 carbon steel substrate

Element	C	Mn	P	S	N	Fe
Content	0.2	1.4	0.05	0.05	0.01	Balance

### 2.2 Preparation of Olive Leaf Extracts

In this study, two types of olive leaf extracts are prepared: extract produced by boiling olive leaves in distilled water and extract produced by boiling olive leaves in 70% ethanol.

### 2.3 Encapsulation

As presented in Table 2, different materials were used for fabrication of submicron capsules. For preparation of the submicron capsules, all the materials listed in Table 2 except ethylene glycol, were dissolved in distilled water with agitation for 30 minutes at 1000 rpm and 70 °C. After complete dissolution, the ethylene glycol was added and agitation was continued under the same conditions for two hours. The mixture was then cooled down to the room temperature, filtered and dried out to produce the capsules filled with both the inhibitor and healing agent.

**Table 2.** The ingredients of capsules and their role in the capsule synthesis and coating.

Material	Application
Urethane Pre-polymer	Capsule Shell wall
HOPDMS	Healing agent
PDES	Healing agent
DBTL	Catalyst
Chlorobenzene	Stabilizer
Arabic gum	Suspending Agent
Ethylene Glycol	Chain Extender
Epoxy Vinyl Ester	Coating Matrix
Benzoyl Peroxide (BPO)	Initiator
Dimethyl Aniline (DMA)	Activator /Adhesion promoter
Ethanol extracted Olive Leaf	Inhibitor

## 2.4 Dispersion of capsules into epoxy and polyurethane and coating applying

Smart coatings were prepared by dispersing 3, 4 and 5 wt% of the synthesized submicron capsules into epoxy and polyurethane resins, followed by mixing suitable hardeners. The mixtures were then degassed and the coating solutions were applied on one side of steel substrates by applicator. Finally, coated samples were cured at room temperature for 24 h.

## 2.5 Electrochemical and Microstructural Tests

Electrochemical impedance spectroscopy (EIS), and potentiodynamic tests were implemented to study the corrosion protection properties of olive leaf extracts as an inhibitor, and coatings containing healing agent. It should be noted that, the quality of the extract was evaluated by comparison of their inhibition performance with commercial olive leaf extract, Oleuropein ( $\geq 98.0$ , sigma Aldrich). Different concentrations of extract including 100, 200, 300, 500 and 1000 ppm were tested to obtain the optimum concentration. Potentiodynamic measurements were carried out by  $\mu$ Autolab type III/FRA2 electrochemical interface potentiostat-galvanostat equipment, connected to a pc. A three electrode system consisting of working electrode, platinum sheet as counter electrode and Ag/AgCl reference electrode was used. 0.6M NaCl in distilled water was used as testing solution and the samples were placed in the solution 24 hours prior the electrochemical tests. The potentiodynamic measurement were conducted in potential range of -0.9 to -0.1 V relative to reference electrode with 1 mm/sec scan rate. EIS measurements were performed in frequency range of 0.1 to 100 KHz in -0.9V potential versus Ag/AgCl reference electrode.

For characterization of fabricated capsules, shell material was extracted by Soxhlet apparatus. Fourier transform infrared spectroscopy (FTIR) spectrum of capsules was recorded on a Bruker spectrometer in  $400-4000\text{ cm}^{-1}$ . Microstructural characterization was carried out by a VEGA\\TESCAN-XMU Scanning electron microscope (SEM).

## 3. RESULTS AND DISCUSSIONS

### 3.1 Inhibition Effect of Olive Leaf Extracts

#### 3.1.1 Electrochemical Tests

In order to investigate the inhibition properties of olive leaf extract on A307 steel in 0.6M NaCl solution, potentiodynamic tests were conducted. The potentiodynamic plots for the three types of inhibitors is shown in Fig. 1-a to 1-c. Table 3 presents the Tafel slopes ( $b_a$  and  $b_c$ ), corrosion potentials ( $E_{\text{corr}}$ ) and corrosion currents ( $I_{\text{corr}}$ ) which were obtained from the potentiodynamic tests. Polarization resistance ( $R_p$ ) can be calculated from Stern-Geary equation:

$$R_p = b_a \cdot b_c / (b_a + b_c)$$

1)

According to Table 3, by increasing the concentration of leaves extract to a certain point in each case,  $R_p$  increases and  $i_{corr}$  decreases which indicates decreasing of corrosion rate. However, further increasing the inhibitor concentration, slightly increases the corrosion rate. In all 3 types of extracts used, with increasing the extract concentration up to about 300 ppm, the corrosion potential shifts toward more positive values, but beyond that concentration, the corrosion potential slightly moves back toward negative direction. This evidence clearly shows that the olive leaf extract controls the steel corrosion by acting as a barrier to mass and charge transfer that kinetically reducing reaction rates, and thermodynamically making the steel nobler in the specified environment. Also, it can be said that this extract acts as a mixed type inhibitor for steel in chloride solutions [12,19,23].

The inhibitor efficiency can be calculated from equation 2:

$$\eta = (i_2 - i_1) / i_1 \tag{2}$$

In this equation,  $i_2$  is the corrosion current after inhibitor addition,  $i_1$  is corrosion current before addition of inhibitor, and  $\eta$  is inhibitor efficiency [15,19,24]. Base on Table 3, in all concentrations of inhibitors, the commercial extract shows the best protection for the steel and ethanol extracted inhibitor shows a better protection than water extracted inhibitor. Higher inhibition efficiency of commercial extract is due to more advanced extraction technology used in industry, producing a high quality extract.

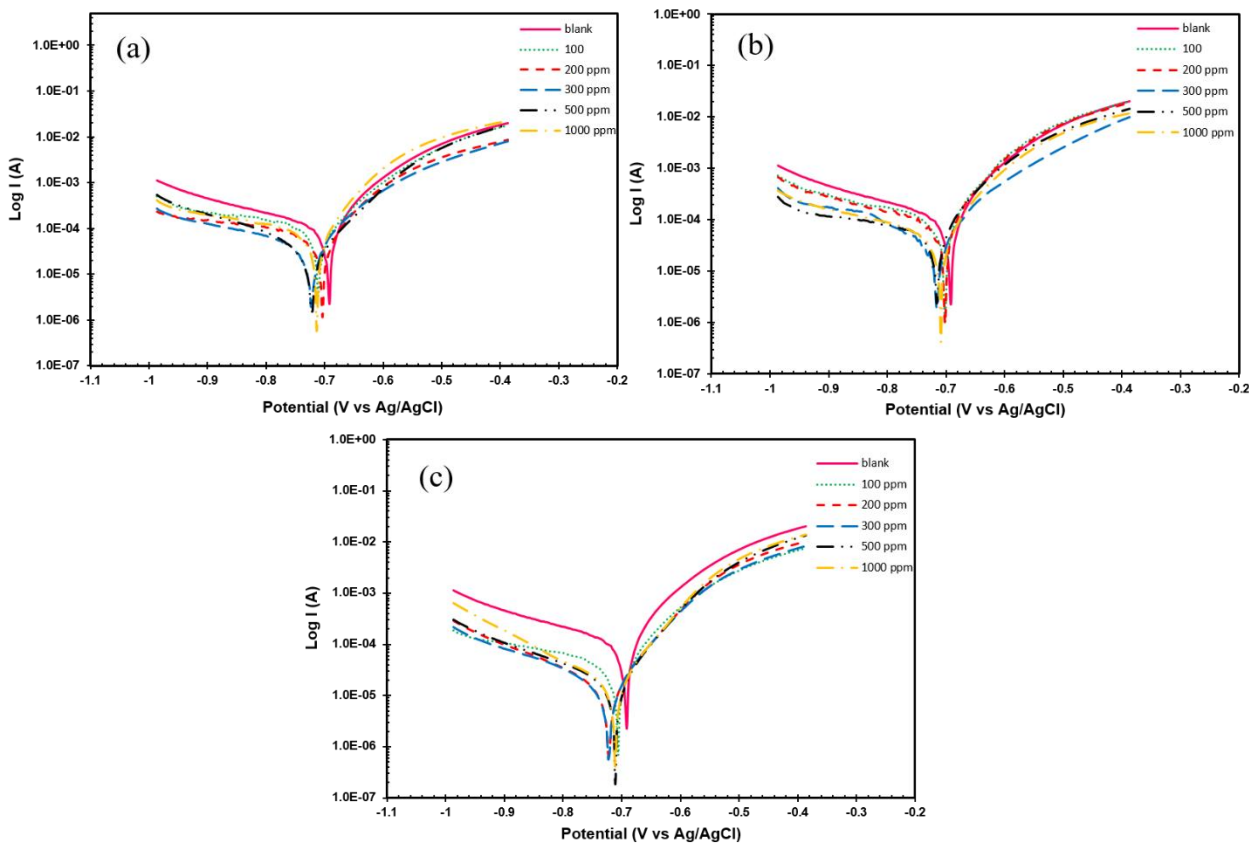


**Figure 1.** Potentiodynamic test results for A37 steel in different concentrations of olive leaf a) extracted by ethanol, b) extracted by water, c) commercial extract.

The optimum performance of the inhibitor in all of extracts, is achieved in a concentration of about 300 ppm, where the maximum inhibition efficiency of commercial, ethanol and water extracted inhibitors is 90.2, 79.7 and 69.4 % respectively. Further increasing inhibitor concentration, does not improve corrosion protection. This behavior can be explained by the fact that the corrosion inhibition is obtained by coverage of the metal surface by an active compound in the inhibitor chemistry. Phenolic compounds present in olive leaves extract, can be absorbed on steel surface and is the main compound responsible for the corrosion inhibition property of these extracts [15,22,25].

**Table 3.** Results of potentiodynamic tests for three types of inhibitors: extracted by water, ethanol and commercial extract

Concentration (ppm)	$b_a$ (mV/dec)	$b_c$ (mV/dec)	$i_{corr}$ ( $\mu Acm^{-2}$ )	$E_{corr}$ (mV <sub>Ag/AgCl</sub> )	$R_p$ ( $\Omega cm^2$ )	$\eta\%$
<b>Blank</b>	95	280	98	-692	67	0.00
<b>Ethanol Extracted</b>						
100	85	230	63	-701	112	33.1
200	70	130	42	-704	169	57.1
300	95	270	19.9	-721	294	79.7
500	80	110	35	-719	263	64.3
1000	65	90	39	-716	245	60.2
<b>Water Extracted</b>						
100	105	140	73	-698	106	25.5
200	105	140	50	-699	158	49.9
300	125	160	30	-719	274	69.4
500	120	150	37	-718	229	62.9
1000	105	150	40	-704	223	59.8
<b>Commercial</b>						
100	75	175	30	-703	129	69.4
200	75	190	12	-718	173	87.3
300	150	65	9	-722	327	90.2
500	65	150	12	-705	261	87.8
1000	75	180	15	-705	273	84.6

Electrochemical impedance spectroscopy (EIS) method was used for evaluating the steel corrosion behavior in presence of different concentrations of ethanol extract. The nyquist plots resulted from EIS are shown in Fig. 2-a. The equivalent circuit corresponding to nyquist plots is shown in Fig.

2-b. The general shape of spectra is a depressed semicircle at high frequencies that attribute to corrosion charge transfer. Since the frequency distribution depends on the surface roughness and inhomogeneities formed during corrosion of metal surface, spectra are not perfect in shape [20,26,27]. By increasing the inhibitor concentration up to 300ppm, the nyquist semi-circle diameter increases, proving that increasing inhibitor concentration to 300ppm, decreases the corrosion damage [13,26,28]. Simulated parameters of the elements in equivalent circuit of Fig. 2-b are represented in Table 4. The Impedance function of a CPE is described in following equation:

$$z=1/Y(iw)^{-n} \quad 3)$$

In which y is proportionality factor,  $i^2=-1$  is imaginary number, w is angular frequency and n is phase shift. In this equation,  $n=0$  describes ideal resistance,  $n=1$  represents ideal capacitance and  $n=-1$  describes ideal inductance [13,27,29]. The deviation from ideal capacitor which is observed in Table 4 is due to formation of surface defects such as inhomogeneities and pores, or adsorption of inhibitor on the surface [23,27]. The relation between double layer capacitance and  $R_p$  is described as below:

$$c_{dl} = 1/[2\pi f_{max}R_p] \quad 4)$$

In which the  $f_{max}$  represents the maximum of angular frequency[20,21]. Based on results of Table 4, Charge transfer resistance,  $R_{ct}$  is increased and  $c_{dl}$  decreases due to adsorption of inhibitor on the metal surface in inhibitor concentrations up to 300 ppm, proving this concentration is the optimum[20,21,27].

Double layer capacitance is described by Helmholtz model (eq. 5):

$$c_{dl}= A\epsilon\epsilon^{\circ}/d \quad 5)$$

$\epsilon^{\circ}$ Is permeability coefficient of air, A is the surface of electrode,  $\epsilon$  is dielectric constant, and d is thickness of electrical double layer[20,26]. Inhibitor adsorption to surface leads to an increase in thickness of electrical double layer (d) and decreases the electrical double layer capacitance. By increasing the inhibitor concentration to 300 ppm,  $c_{dl}$  decreases, meaning the adsorption of inhibitor to metal surface and consequently thickness of adsorbed layer increases. However, above this concentration the  $c_{dl}$  decreases, implying inhibitor desorption[20,26]. This observation is in agreement with potentiodynamic results.

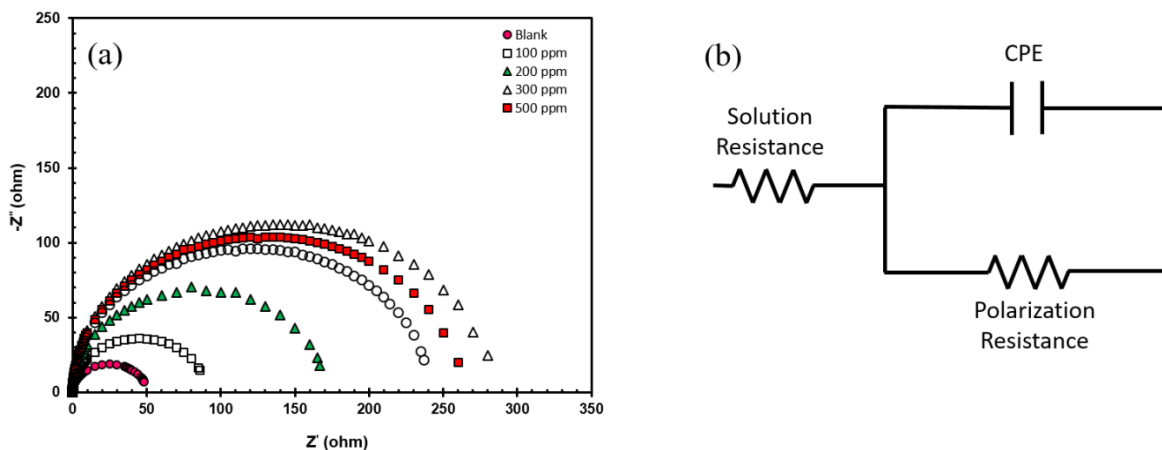


**Figure 2.** a) Nyquist plot of steel in 0.6 M NaCl containing 0, 100, 200, 300, 500 and 1000 ppm olive leaf extracted by ethanol as an inhibitor and b) the equivalent circuit.

**Table 4.** Fitting of Nyquist plots of steel in 0.6 M NaCl containing 0, 100, 200, 300, 500 and 1000 ppm olive leaf extracted by ethanol as an inhibitor on equivalent circuit described in Fig. 2-b.

Sample	$R_s$ ( $\Omega\text{cm}^2$ )	CPE		$R_{ct}$ ( $\Omega\text{cm}^2$ )	$C_{dl}$ ( $\mu\text{F cm}^{-2}$ )
		$Y_0$ ( $\Omega\text{ s}^n\text{cm}^{-2}$ ) $\times 10^{-6}$	n		
Blank	16.3	88.2	0.90	48.2	350.3
100 ppm	16.5	83.5	0.85	91.5	220.6
200 ppm	18.1	79.0	0.87	173.7	193.2
300 ppm	17.9	72.3	0.91	281.1	101.5
500 ppm	17.0	76.6	0.89	260.5	148.9
1000 ppm	16.2	75.8	0.91	234.0	170.3

### 3.1.2 Adsorption isotherm

In order to analyze the interaction between the inhibitor molecules and the steel surface, various adsorption isotherms (Temkin, Frumkin, Freundlich, and Langmuir) were examined to find out which one better fits the surface coverage values ( $\theta$ ) at different concentrations of inhibitor. Surface coverage is obtained from equation 6:

$$\theta = \eta / 100 \tag{6}$$

In which the  $\eta$  shows the inhibition efficiency[18,19]. The dependence of  $C/\theta$  to  $C$  for olive leaves extracted by ethanol is shown in Fig. 3, where  $\theta$  is the fractional surface coverage and  $C$  is the inhibitor concentration. A straight line was fitted using the least squares method to calculate the adsorption parameters. Calculated regression coefficient close to unity (0.9988), shows the

experimental data are well described by Langmuir isotherm with a single layer adsorption mechanism, given by the equation:

$$\theta/(1-\theta) = k_{\text{ads}}C \quad (7)$$

Where  $k_{\text{ads}}$  is the equilibrium constant of the adsorption process [22,27]. In this isotherm no interaction between the adsorbed molecules is assumed [18,19,22].

Free adsorption energy in standard mode can be evaluated from the following equation [15,22]:

$$\Delta G_{\text{ads}}^{\circ} = -RT \ln(55.5k_{\text{ads}}) \quad (8)$$

According to this equation, the inhibitor absorption energy can be presented as below:

$$\Delta G_{\text{ads}}^{\circ} = -18.757 \text{ kJ mole}^{-1} \quad (9)$$

The negative value of standard adsorbing free energy indicates spontaneous adsorption of inhibitor molecules on the steel surface. Inhibitor molecules can be adsorbed on metal surface by physical or chemical interactions. When the absorption energy is lower than  $-40 \text{ kJ mole}^{-1}$ , adsorption is assumed to be chemical and when the absorption energy is higher than  $-20 \text{ kJ mole}^{-1}$  adsorption is assumed to be physical. According to this assumption, the adsorption of olive leaf extract on the steel surface in 0.6M NaCl solution is physical [12,19,22].

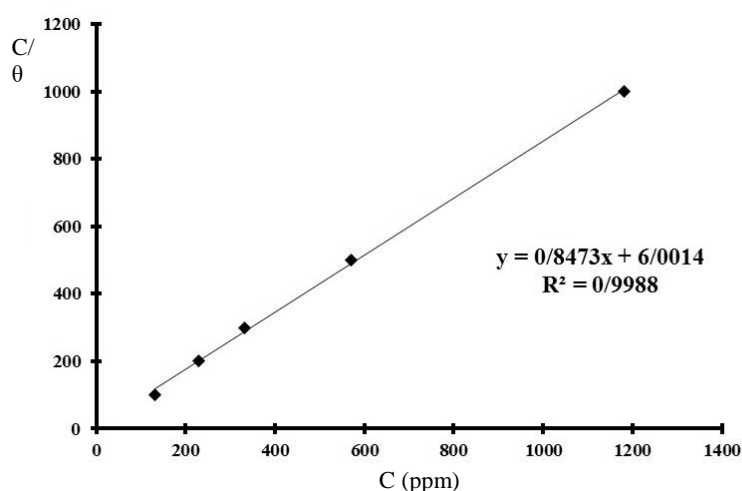


**Figure 3.** Langmuir adsorption isotherm for inhibition of olive leaves extracted by ethanol.

### 3.2 Capsules Characterization

SEM images of synthesized capsules are shown in Fig. 4-a and 4-b. The average size of the capsules is estimated to be below  $1 \mu\text{m}$  which is highly dependent on agitation intensity (sonication process) because it transports the ultrasonic energy to the solution and small capsules [3]. Based on Fig.

4-b, the capsules surface seems to be rough. EDS analyzes of one of the capsules is shown in Fig. 4-c and the chemical composition obtained from the EDS is presented in Table 5. Shown in this table, presence of C and O as the most abundant elements, confirms the formation of urethane as shell of capsules[30].

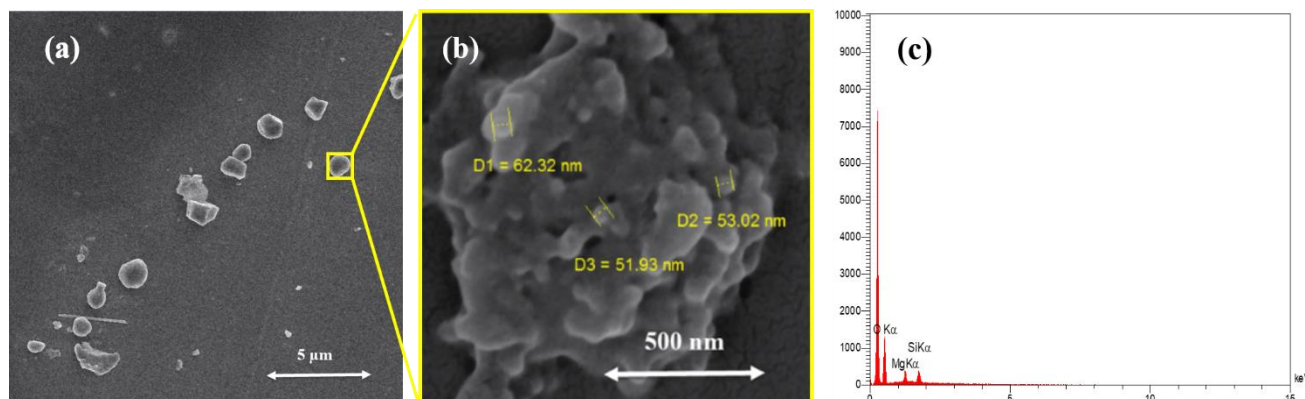


**Figure 4.** SEM images of a) fabricated capsules, b) surface roughness of capsules at higher magnifications and c) EDS spectra of a capsule.

**Table 5.** EDS analysis results of capsules shown in Figure. 4-c

element	Atomic percent	Weight percent
<b>C</b>	73.69	66.30
<b>O</b>	23.39	28.03
<b>Mg</b>	1.65	3.01
<b>Si</b>	1.26	2.66

FTIR analyzes was used for characterization of the shell material. The FTIR spectra is shown in Fig. 5, in which the N-H strengthening vibration at  $3416.4\text{ cm}^{-1}$ , the C-H strengthening vibration at  $2598.18$ ,  $2925.88$  and  $2855.12\text{ cm}^{-1}$ , the C=O strengthening vibration at  $1606.91\text{ cm}^{-1}$ , and C-O-C strengthening vibration at  $1079.72$  and  $1035.73\text{ cm}^{-1}$  are observed. From these evidences, it can be concluded that the shell material is urethane[30,31].

### 3.3. Coating Behavior

#### 3.3.1 Self-healing behavior

SEM images of self-healing process of epoxy coatings containing 3 and 5 wt% of capsules after 24 h immersion in 0.6M NaCl are shown in Fig. 6. When the coating is cracked due to an external force, the healing agent/inhibitor containing submicron capsules are also cracked and the healing and inhibitor

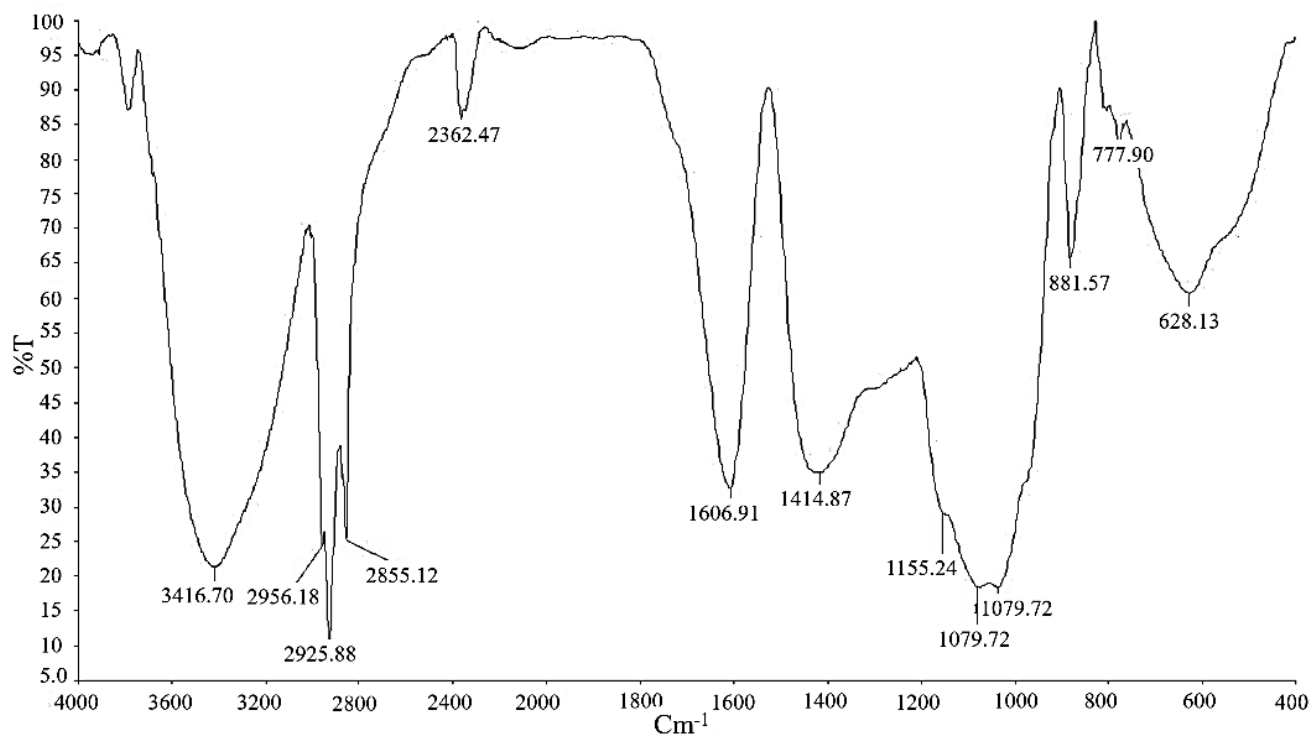


**Figure 5.** FTIR spectra of the synthesized capsules.

compounds are released [3,6]. As seen in Fig. 6-a and 6-b, in 3 wt% capsule containing coatings, the cracks are not healed properly and corrosion products can be seen in the cracked areas due to diffusion of NaCl solution to the metallic substrate. However, in the coating containing 5 w% capsule (Fig. 6-c and 6-d), the cracks are seen to be healed effectively and no evidence of corrosion adjacent to cracked area can be observed. Fig. 7 shows the proposed self-healing mechanism of coating. According to this image, when a crack is formed in the coating, some capsules are destroyed and release their content (self-healing agent and inhibitor) and reduce the corrosion damage by recovering the coating and chemically protecting the metal surface. Following that, adjacent capsules release their content and healing the coating [32-34].

The effect of particle size on the self-healing behavior have been studied by Rule [28]. In this research, it is stated that increasing the size of the capsules, enhances the performance of self-healing coating due to higher amount of healing agent that can be released. However, in other studies using submicron and nano-sized capsules, it is concluded that self-healing is improved by decreasing particles size, because the particles can diffuse to the pores and cracks surfaces and heal the damaged area. This mechanism is proven to be true in both simulation models [35,36] and experimental studies [37].

Particles migrate to cracks walls due to the attraction of particles to open surfaces. With particle size decreasing, the diffusion process will be accelerated and the cracks will be disclosed faster [37].

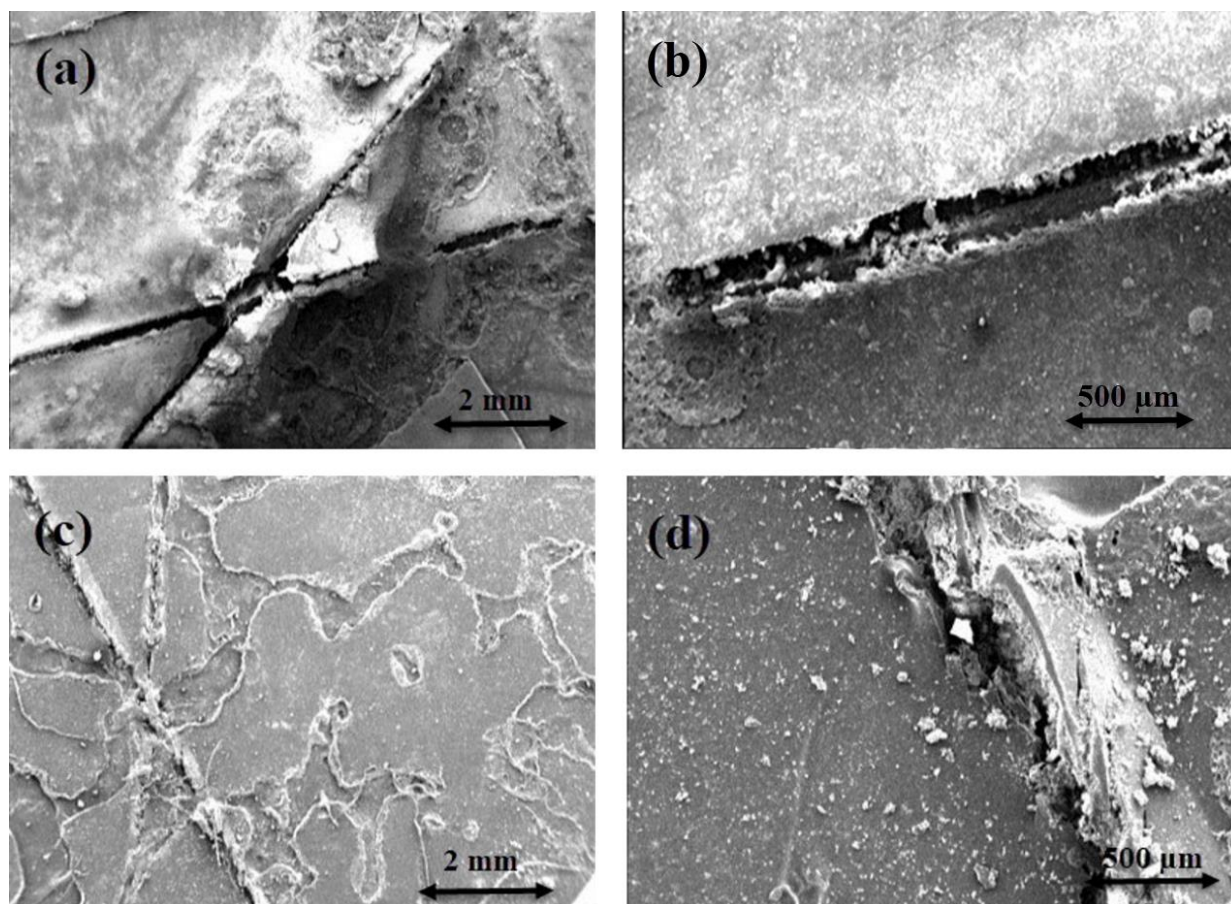


**Figure 6.** SEM images of artificial scratch on epoxy coating containing a, b) 3 wt% and c, d) 5 wt% capsules after 24 h immersion in 0.6M NaCl.

### 3.3.2 Electrochemical Studies of the coating

Potentiodynamic tests were conducted for investigation of self-healing process in scratched epoxy and polyurethane coatings containing 0, 3, 4 and 5 percent of capsules. Samples with scratched coatings were placed in 0.6M NaCl solution for 24 hours before testing. The results obtained from potentiodynamic tests is illustrated in Fig. 8. The coated and scratched sample without the capsules, shows a high corrosion current density ( $10 \mu\text{Acm}^{-2}$  and  $20 \mu\text{Acm}^{-2}$  for epoxy and polyurethane coatings, respectively) meaning a low corrosion resistance. On the other hand, in the samples with capsule containing coating, resistance to corrosion is considerably higher ( $0.9 \mu\text{Acm}^{-2}$  and  $2 \mu\text{Acm}^{-2}$  for epoxy and polyurethane coatings with 5 percent of capsules, respectively) and by increasing the amount of capsules in the coating, the corrosion current density reduces and resistance to corrosion increases. The corrosion resistance of samples with capsules containing coatings is affected by two factors: self-healing property of the coating due to presence of capsules, and corrosion inhibition of olive leaves extract embedded inside the capsules[38,39].

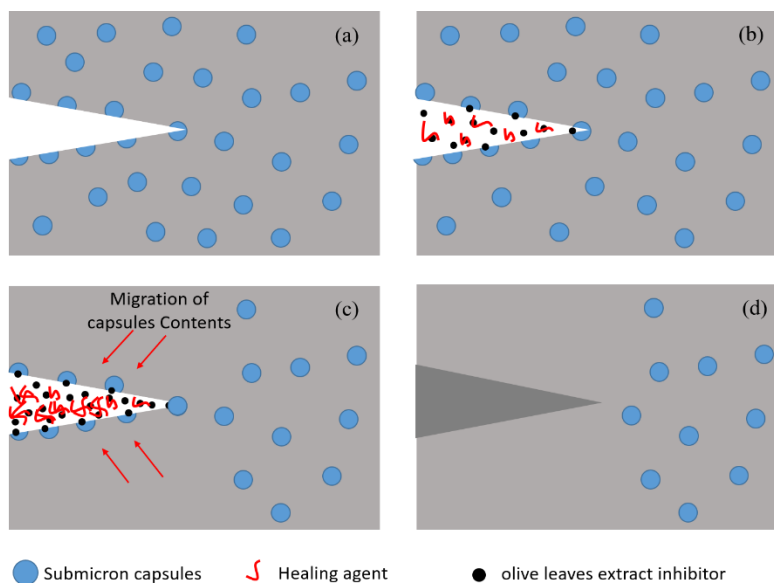


**Figure 7.** A schematic of self-healing mechanism by capsules, a) destruction of capsules due to crack b) release of the capsules content (self-healing agent and inhibitor), c) migration of adjacent capsules content to crack wall and d) crack healing.

A perfect coating on the metal surface, acts as a capacitor and protects the metal by banning the electrical current. In the coatings with no healing agents, when the coating is scratched, the substrate metal will be in contact with the environment and an electric circuit is formed. By forming a circuit, the corrosion of the metal continues with no prevention. Alternatively, in the coatings containing capsules, by scratching the coating, healing agents are released and a new coating is formed on the metal surface. Yet, the newly formed coating is not flawless and some pores and defects remain in the healed area. In this case, the corrosion inhibitor embedded in the capsules play its role and protects the bare metal by adsorbing to metal surface[7,38,39].It should be noted that the increase in corrosion resistance with capsule content is not equal in different coatings, and epoxy shows a better performance in comparison to polyurethane coatings.

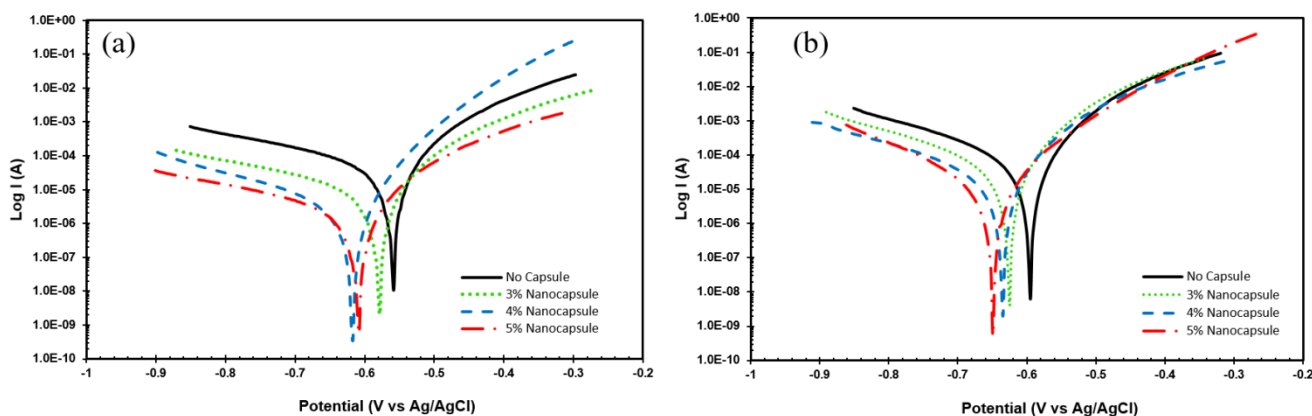


**Figure 8.** Potentiodynamic results of embedded coatings with 0, 3, 4 and 5 wt% of capsules, a) epoxy coating and b) polyurethane coating.

Electrochemical impedance spectroscopy (EIS) analyzes was carried out for studying the self-healing mechanism of the coatings. Equivalent circuit for EIS modeling is shown in Fig. 9-a. Bode, phase, and Nyquist plots for epoxy coatings containing 3, 4, and 5 percent of capsules, and for polyurethane coating with 3 percent capsules are depicted in Fig. 9-b to 9-d respectively. In Fig. 9-b, the depressed, capacitive-like semicircle, indicates that the corrosion process is under charge transfer control. Also, the nyquist plots shown in Fig. 9-b specify that increasing amount of capsule contents increases diameters of the semicircles and impedance of the interface in full frequency range that means increasing the corrosion resistance. Liu and Chen investigated embedding of sodium tungstate loaded talcum powder into an epoxy-resin coating to create a new anticorrosive and self-healing coating for metallic substrates. They reported that the arc radius of nyquist diagram increased by one order of magnitude compared to the blank samples which means that the modified coating protects the metal matrix from corrosion [29]. Horizontal part of bode diagram in Fig. 9-c is related to charge transfer resistance of coating and this amount increases with addition of capsule content [9,40,41]. From Fig. 9-d it is evident that increasing capsule content don't change phase angle plot, and the maximum phase angles of all samples appear at a frequency between 10 to 100 Hz, while all the maximum phase angles are about  $-80^\circ$ . Based on Fig. 9-b, impedance and corrosion resistance of epoxy coated sample with 3 wt% capsules is clearly higher than polyurethane coated with same amount of capsules which can be related to higher healing ability in epoxy coatings[38,42]. The results are consistent with the results obtained from potentiodynamic tests.

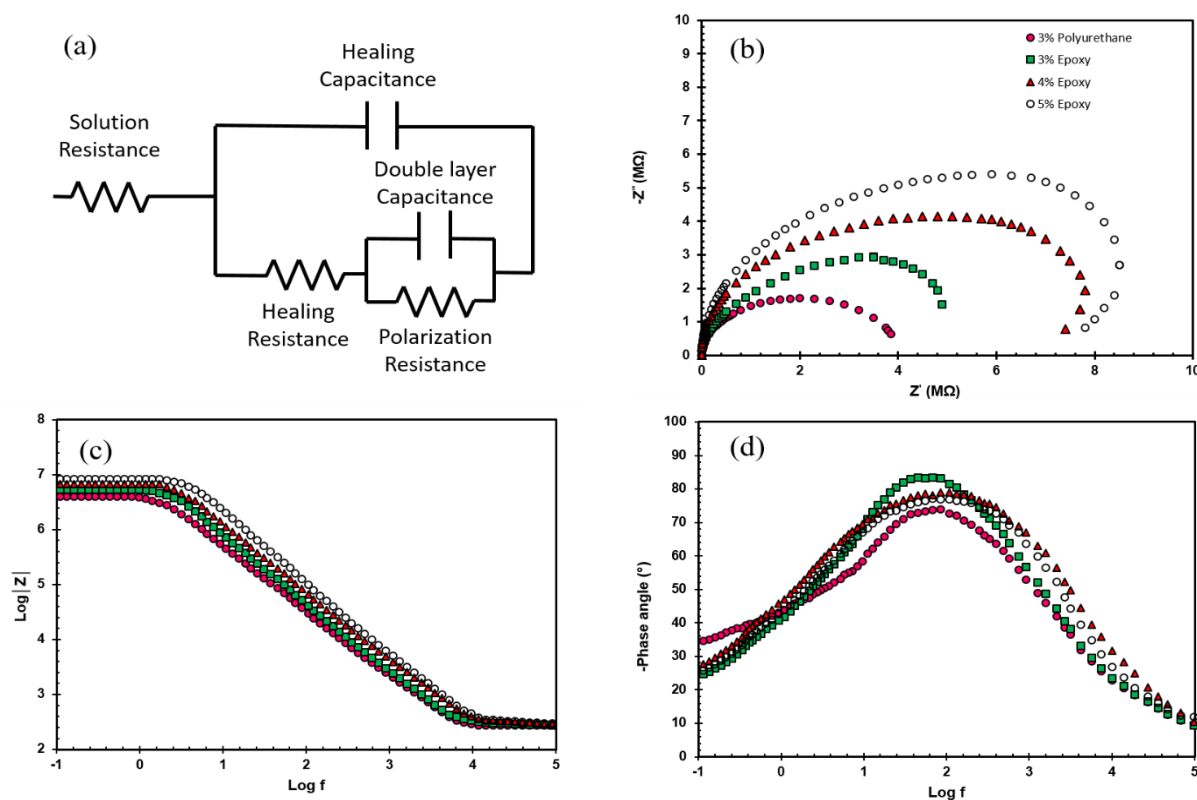


**Figure 9.** EIS results of the epoxy coated samples with 0, 3, 4 and 5 wt% and polyurethane coated sample with 3 wt% of capsules, a) equivalent circuit, b) nyquist plot, c) bode plot and d) phase plot.

#### 4. CONCLUSION

In the present research, extracts of olive leaf as a green inhibitor was studied and the behavior of coatings containing inhibitor and healing agent embedded capsules was investigated.

The ethanol extracted inhibitors, proved to be effective inhibitor with about 80% inhibition efficiency for steel in chloride solution at 300 ppm concentration of inhibitor. Capsules containing inhibitor and healing agent were synthesized by agitation assisted sonication. The capsules were observed by SEM and it was found out that the average capsules size is below 1  $\mu\text{m}$ .

The behavior of damaged coating was investigated with microscopy. It was shown that in presence of 5 wt% healing agent and inhibitor containing capsules, the corrosion attack is hindered in the adjacent area of the damage. With increasing capsule content in the coating, the corrosion protection properties of the coating improves, so that the best protection is achieved with epoxy coating containing 5 wt% of capsules.

#### ACKNOWLEDGEMENTS

The authors would like to thank the Sharif University of Technology for the financial support provided during the course of this research.

#### References

1. Y. González-García, J.M.C.Mol, T. Muselle, I. De-Graeve, G. Van-Assche, G. Scheltjens, B. Van-Mele and H. Terryn, *Electrochem. Commun.*, 13 (2011) 169.
2. M. Samadzadeh, S. Hatami-Boura, M. Peikari, A. Ashrafiand M. Kasiri, *Prog. Org. Coat.*, 70 (2011) 383.
3. M. Samadzadeh, S. Hatami-Boura, M. Peikari, S.M. Kasirihaand A. Ashrafi, *Prog. Org. Coat.*, 68 (2010) 159.
4. T. Nesterova, K. Dam-Johansenand S. Kiil, *Prog. Org. Coat.*,70 (2011) 342.
5. T. Yin, M.Z. Rong, M.Q. ZhangandG.C.Yang, *Compos. Sci. Technol.*,67 (2007) 201.
6. B.J. Blaiszik, N.R. Sottosand S.R. White, *Compos. Sci. Technol.*,68 (2008) 978.
7. M. Huang, H.Zhangand J. Yang, *Corrosion Science*,65 (2012) 561.
8. C. Suryanarayana, K.C. Raoand D. Kumar, *Prog. Org. Coat.*,63 (2008) 72.
9. M. Behzadnasab, S.M. Mirabedini, M. Esfandehand R.R. Farnood, *Prog. Org. Coat.*,105 (2017) 212.
10. S.M. Mirabedini,I.Dutiland R.R.Farnood, *Colloids Surf. A.*, 394 (2012) 74.
11. M.L. Zheludkevich, K.A. Yasakau, A.C. Bastos, O.V. KaravaiaandM.G.S. Ferreira, *Electrochem. Commun.*, 9 (2007) 2622.
12. T. Ibrahim, H. Alayanand Y. Al-Mowaqet, *Prog. Org. Coat.*, 75 (2012) 456.
13. A. Yakubiand T. Nishinika, *Corrosion Science*, 53 (2011) 4118.
14. S.V. Lamaka, M.L. Zheludkevich, K.A. Yasakau, R. Serra, S.K. PoznyakandM.G.S. Ferreira, *Prog. Org. Coat.*, 58 (2007) 127.
15. A.Y. El-Etre, *Corrosion Science*, 45 (2003) 2485.
16. A.M. Abdel-Gaber, B.A. Abd-El-Nabey, E. KhamisandD.E. Abd-El-Khalek, *Desalination*, 278 (2011) 337.
17. P.C. Okafor, M.E. Ikpi, I.E. Uwah, E.E. Ebenso, U.J. Ekpeand S.A. Umoren,*Corrosion Science*, 50

- (2008) 2310.
18. E.A.Noor, *Int. J.Electrochem. Sci.*, 12 (2007)996.
  19. A.Y. El-Etre, *J. Colloid Interface Sci.*, 314 (2007) 578.
  20. S. Dengand X. Li, *Corrosion Science*, 55 (2012) 407.
  21. A. Bouyanzer, B. Hammoutiand L. Majidi, *Mater. Lett.*, 60 (2006)2840.
  22. S. Pauland I.Koley, *J. Bio- and Tribo- Corrosion*, 2 (2016) 2.
  23. C. Rahal, M.Masmoudi, R.Abdelhedi, R. Sabot, M.Jeannin, M.Bouaziz and P.Refait, *J.Electroanal. Chem.*, 769 (2016) 53.
  24. A.T.Simonović, M.B.Petrović, M.B.Radovanović, S.M. MilićandM.M. Antonijević, *Chemical papers*, 68 (2014)362.
  25. F.S. de Souzaand A.Spinelli, *Corrosion science*, 51 (2009)642.
  26. M.P. Desimone, G. GordilloandS.N. Simison, *Corrosion Science*, 53 (2011)4033.
  27. W.Li, Q. He, S.Zhang, C.Pei andB. Hou, *J. Appl.Electrochem.*, 38 (2008)289.
  28. J.D. Rule, N.R. SottosandS.R. White, *Polymer*, 48 (2007), 3520.
  29. Y. LiuandY. Chen, *Int. J.Electrochem. Sci.*, 13 (2018)530.
  30. B. Di-Credico, M. Leviand S.Turri,*J.Eur-Polym.*, 49 (2013)2467.
  31. A.M.Atta, A.M.El-Saeed, H.I.Al-ShafeyandG.A.El-Mahdy, *Int. J.Electrochem. Sci.*, 11(2016)5735.
  32. E.M.Fayyad, M.A.Almaadeed, A. JonesandA.M.Abdullah, *Int. J.Electrochem. Sci.*,9 (2014) 4989.
  33. S.H. Cho, S.R. WhiteandP.V. Braun, *Adv. Mater.*,6 (2009)645.
  34. K. Wazarkar, D. Patil, A. Rane, D. Balgude, M. KathalewarandA. Sabnis,*RSC Advances*, 108 (2016)106964.
  35. J.Y.Lee,G.A. BuxtonandA.C. Balazs, *J. Chem. Phys.*, 121 (2004) 5531.
  36. S. Tyagi, J.Y. Lee, G.A.BuxtonandA.C. Balazs,*Macromolecules*,37 (2004) 9160.
  37. S.Gupta, Q.Zhang,T.EMRICK,A. BalzasandT. Russel, *Nat.Maer.*, 5 (2006) 229.
  38. 38.P. VijayanandM.A. AlMaadeed, *Express Polym.Lett.*,6 (2016) 438.
  39. A. Lutz, O. van-den-Berg, J. Wielant, I. De-GraeveandH. Terryn, *Frontiers in Materials*,2 (2016) 73.
  40. 40.D.A.Leal,I.C.Riegel-Vidotti,M.G.S. FerreiraandC.E.B.Marino,*Corrosion Science*, 130 (2018) 56.
  41. 41.R.Najjar, S.A. KatouraniandM.G. Hosseini,*Prog. Org. Coat.*, 124 (2018)110.
  42. 42.Y.C. Yuan, M.Z.Rong, M.Q. Zhang, J. Chen, G.C. YangandX.M.Li, *Macromolecules*, 14 (2008)5197.